Korean J. Chem. Eng., 36(1), 101-108 (2019)
DOI: 10.1007/s11814-018-0168-8

pISSN: 0256-1115
eISSN: 1975-7220

Adsorption and precipitation of anionic dye Reactive Red 120 from aqueous solution by aminopropyl functionalized magnesium phyllosilicate

Yong-Woon Kim*, Jung-Hun Kim*, Deok Hyun Moon, and Hyun-Jae Shin*,†**

*Department of Biochemical and Polymer Engineering, Chosun University, 309 Pilmundaero, Dong-gu, Gwangju 61452, Korea
**Department of Environmental Engineering, Chosun University, 309 Pilmundaero, Dong-gu, Gwangju 61452, Korea
(*Received 15 August 2018 • accepted 10 October 2018*)

Abstract−Dye wastewater causing destruction in ecosystem from a variety of plants an operation needs various factors for environmental cleanup. To improve removal efficiency of dye wastewater, various adsorbents including clay and nonclay-related materials have been tried. The use of soluble aminopropyl functionalized magnesium phyllosilicate (Mg-AMP clay) as an adsorbent for the textile anionic dye Reactive Red 120 (RR 120) was examined thermodynamically and kinetically. The adsorption kinetics followed the pseudo-second-order and Langmuir isotherm equation fitted best models. A maximum amount of adsorption was determined to be 229.9 mg/g, which is one of the highest values studied so far. An Mg-AMP clay dosage of 10 mg/mL obtained from Langmuir model a maximum adsorption capacity of 229.94, 182.26 and 156.54 mg/g at 298.15, 308.15 and 318.15 K, respectively. Moreover the thermodynamic activation parameters such as enthalpy and entropy were determined. We suggest the removal mechanism of RR 120 using Mg-AMP clay by adsorption and precipitation.

Keywords: Anionic Dyes, Magnesium Phyllosilicate, Clay, Adsorption, Precipitation, Reactive Red 120

INTRODUCTION

Environmental cleanup is mainly focused on the removal of contaminants from polluted industrial wastewater, which destroys the ecosystem. In particular, the textile industry includes many types of processing [1]. Textile dyes can be considered as emergent contaminants in water and can contribute the mutagenicity of representative environmental samples [2]. Reactive dye is a dye that can react directly with the fabric, which means that a chemical reaction transpires between the dyes and the molecules of the fabric, effectively making the dyes a part of the fabric [3]. Reactive Red 120 (RR 120) is widely used for textile dyeing in many countries such as Brazil and Tunisia [4]. Most of the dyes can cause an allergic skin reaction, such as allergy, dermatitis, and skin irritation, and are therefore considered as hazardous materials and toxic compounds for humans [5-7]. To remove the dye from an aqueous solution, many chemical processes, including adsorption process, as well as biological process have been applied to wastewater [8,9]. In the adsorption process for the removal of pollutants from wastewater, activated carbon is usually used as an adsorbent because of its high adsorption capacity, low cost, and simplicity of process [10]. For the adsorption process, various other adsorbents have also been used, which are as follows: chitosan [11], polystyrene anion exchange resin [12], Fe_3O_4 magnetic nanoparticles [13], oxygen furnace slag [14], and Fouchana clay [15,16]. Among them, clays are used in industrial applications because of its low cost and natural productivity [17]. For this reason, various industries consume large amounts of raw and synthetic clays [18,19]. Aminopropyl functionalized magnesium phyllosilicate (Mg-AMP clay), which is one of the major synthetic clays, is cationic and water soluble; it has a 2 : 1 trioctahedral structure, resembling the talc-like $Si_8Mg_6O_{20}(OH)_4$ [20]. It is synthesized by a sol-gel method with changes in the chemical conditions to that for metal ions, such as nickel, zinc, calcium, cobalt, copper, ferric and aluminum ions [21,22]. Interestingly, Mg-AMP clay has organic chains of clay sheets, and these organic chains exhibit positive charge by protonated amino groups [23]. Although Mg-AMP clay has been used for many biological and environmental applications [24], to the best of our knowledge, there is no report available in detail on the adsorption of RR 120 using a water-soluble adsorbent such as Mg-AMP clay so far. In this study presents a method for the efficient removal of anionic RR 120 from an aqueous solution using nano-sized Mg-AMP clay prepared by the sol-gel method. The clay enhances the performance of the process by adsorption and precipitation. The adsorption thermodynamics and kinetics are studied, including isotherm and parameter estimation such as enthalpy and entropy. In addition, a removal mechanism is suggested, and the potential applicability in a large-scale implementation is discussed.

EXPERIMENTAL

1. Materials

The anionic dye, Reactive Red 120 (RR 120) was provided by Sigma-Aldrich Chemicals (St Louis, MO, USA) and used without further purification. Its formula is $C_{44}H_{30}Cl_2N_{14}O_{20}S_6$, and the physical properties of RR 120 are given in Table 1. For the treatment experiments, dye solutions with concentrations in the range of 5-100 mg/L were prepared by continuous dilution of the stock solu-

†To whom correspondence should be addressed.
E-mail: shinhj@chosun.ac.kr

Table 1. Physicochemical properties of Reactive Red 120 used in this study

Textile dye	RR 120
Color index name	Reactive Red 120
Molecular formula	$C_{44}H_{24}Cl_2N_{14}Na_6O_{20}S_6$
Molecular weight (g/mol)	1469.98
λmax (nm)	535
C.I. number	292775
Class	Diazo(-N=N- bond)
Charge	Negative
Molecular structure	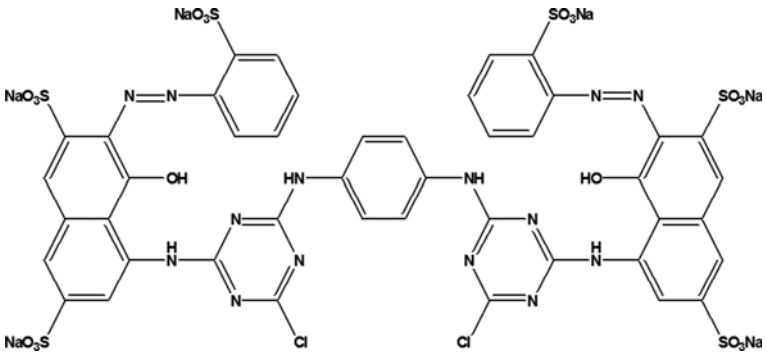

tion with distilled water. The pH of the RR 120 dye solution was adjusted by drop-wise addition of 1 M HCl or NaOH and measured using a pH meter (Docu-pH meter, Sartorius, USA).

3-Aminopropyl triethoxysilane (APTES, 99%) was provided by the Sigma-Aldrich Chemicals (St Louis, MO, USA) and used without further purification. Aminoproyl magnesium phyllosilicate (Mg-AMP clay) was prepared as follows [25-27]. APTES 1.3 mL (5.63 mmol) was added drop-wise to an magnesium chloride 0.84 g (8.82 mmol) and then dissolved in 20 g of ethanol. The precipitated white slurry was stirred overnight. The obtained precipitate was isolated by centrifugation, refined with ethanol (50 mL) three times, and then dried overnight at 40 °C.

2. Characterization

The elemental content (Mg and Si) of Mg-AMP clay was measured using X-ray fluorescence (ZSX100e, Rigaku, Japan). Powder X-ray (X'Pert PRO Multi Purpose X-Ray Diffractometer, PANalytical, Netherlands) patterns were obtained using a Cu-Kα radiation generator operated at 40 kV, 30 mA. The samples was scanned from 3 to 65° at a rate of 1.2° 2θ/min. Fourier transform infrared (FT-IR; Nicolet 6700, Thermo electron, USA) spectra of the Mg-AMP clay, RR 120 and Mg-AMP clay adsorption mixtures, and RR 120 spectra were recorded between 4,000 and 540 cm^{-1} were using the KBr pellet technique. An analysis of the surface characteristics of the adsorbate materials was conducted using scanning electron microscope (Fe-SEM; JSM-7500F, Japan) and energy dispersive X-ray (EDX; X'pert pro MRD, Holland). The effect of adsorption correlation between the adsorbent and the adsorbate materials was evaluated using a UV/Vis spectrophotometer at 535 nm (Ultrospec 2100 Pro, Amersham Biosciences, USA).

3. Isotherm Experiment

To perform the experiments for the evaluation of the adsorption isotherms of RR 120, 10 mg/mL of Mg-AMP clay was added to conical tubes containing 50 mL of dye solution with concentrations between 5 and 100 mg/L. These conical tubes were agitated on a shaking incubator at 130 rpm for 120 min to ensure equilibrium. After that, the samples were centrifuged at 3,000 rpm for 20 min in order to precipitate the adsorption substances. The concentration of RR 120 dye in the supernatant liquid was determined by a spectrophotometer at 535 nm. The amount of RR 120 dye that is adsorbed for the adsorbent at equilibrium is obtained as follows:

$$q_e = \frac{(C_0 - C_e)V}{m} \quad (1)$$

where q_e is the equilibrium amount of adsorption (mg/g), V (L) is the volume of the treated sample, C_0 and C_e (mg/L) are the initial and equilibrium RR 120 concentrations in the liquid phase, and m (g) is the amount of Mg-AMP clay.

4. Modelling of Adsorption Isotherms

Several theories of adsorption equilibrium were applied for the analysis of equilibrium adsorption data that was obtained. The measurement data fit well with both the Langmuir and Freundlich isotherm models, since the constant values of the average percentage error (%) are close to 1.

The mathematical expression of the Langmuir isotherm is given by the following equation [28]:

$$q_e = \frac{q_m b C_e}{1 + b C_e} \quad (2)$$

where q_e (mg/g) is the amount adsorbed at equilibrium, q_m (mg/g) is the maximum amount adsorbed, b (L/mg) is the constant related to the rate of adsorption, and C_e (mg/L) is the equilibrium concentration.

For the Freudlich model, this equation is also applicable to multilayer adsorption and is given as follows [29]:

$$q_e = K_F C_e^{1/n} \quad (3)$$

where K_F is the Freundlich constant, which indicates the adsorption capacity, n is the heterogeneity factor, and 1/n is a measure of the intensity of adsorption. These are calculated from the slope and intercept of the Freundlich plot.

5. Kinetics Experiment

Experiments were conducted to evaluate the effect of temperature on RR 120 adsorption at 293.15, 303.15, and 313.15 K with dye concentration of 5, 10, 15, 20, 30, 50, 60, 70, and 100 mg/L. RR 120 dye solutions with different concentrations were prepared in 50 mL conical tubes. 30 mL of RR 120 solution and 10 mg/mL of Mg-AMP clay were mixed in hermetic 50 mL conical tubes. These conical tubes were kept in each temperature and speed (130 rpm) operating at shaking incubator. The samples were taken after 120 min and centrifuged at 3,000 rpm for 20 min. To evaluate the effect of temperature on the removal of RR 120 from the experimental wastewater, three degrees of temperature were considered: 293.15 K, 303.15 K, and 313.15 K.

6. Modelling of Kinetics

For the study of adsorption thermodynamics, 30 mL of RR 120 solution and 10 mg/L of Mg-AMP clay were mixed in hermetic 50 mL conical tubes. The conical tubes were kept in a shaking incubator. Thermodynamics experiments were conducted by agitating RR 120 solutions of different concentrations: 5-100 mg/L. The thermodynamic parameters of Gibbs free energy (ΔG^o), entropy (ΔS^o), and enthalpy (ΔH^o) were determined using the following equations [30].

$$\Delta G^o = \Delta H^o - T\Delta S^o \quad (4)$$

$$\Delta G^o = -RT \ln K \quad (5)$$

where K is the equilibrium constant of adsorption, T is the temperature of the solution in Kelvin (K), and R is the gas constant (8.314 J/mol K^{-1}). After a suitable period of time, the samples were collected from the supernatant liquid after centrifugation and its absorbance was recorded using UV-Vis spectrophotometer.

For the pseudo first and pseudo second order kinetic models, equations for the liquid solution adsorption system were used. The pseudo-first-order equation is as follows [31]:

$$\frac{dq}{dt} = k_1(q_e - q) \quad (6)$$

$$\log(q_e - q) = \log q_e - \frac{k_1}{2.303}t \quad (7)$$

where k_1 (min^{-1}) is adsorption rate constant.

The pseudo-second-order equation is as follows [32]:

$$\frac{dq}{dt} = k_2(q_e - q)^2 \quad (8)$$

$$\frac{t}{q_t} = \frac{1}{h} + \frac{t}{q_e} \quad (9)$$

$$h = k_2 q_e^2 \quad (10)$$

where k_2 (g/mg min^{-1}) is the pseudo second-order rate constant, which is determined by plotting t/q_t against t.

Table 2. Chemical analysis of fractions of Mg-AMP clay

Chemical composition	Weight (%)
SiO_2	72.2
MgO	22.9
Cl	4.79
Al_2O_3	0.025
Fe_2O_3	0.0077
CuO	0.0062
CaO	0.0056
NiO	0.0041
Br	0.0030
SO_3	0.0014
Total	100

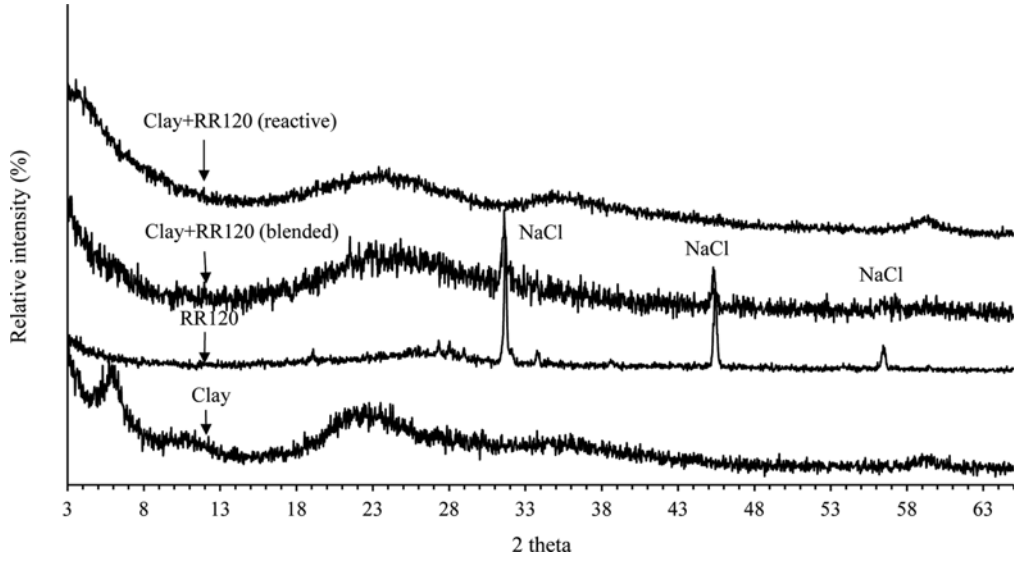

Fig. 1. XRD pattern of Mg-AMP clay before, and after adsorption (clay+RR 120), RR 120 dye.

RESULTS

1. Characterization of Adsorbent, Adsorbate, and Mixture

The XRF instrumental analysis results of the Mg-AMP clay is as follows. The Mg-AMP clay is mostly composed of SiO_2 72.2 wt%, MgO 22.9 wt%, and Cl 4.79 wt% (Table 2). The XRD patterns of the synthesized Mg-AMP clay, RR 120, Clay-RR 120 mixture (blended), and reactive Clay-RR 120 mixture are presented in Fig. 1. Halite (NaCl) was observed as the crystalline phase in RR 120 and aminoclay-RR 120 mixture (blended). However, halite was not observed in the reactive mixture of aminoclay and RR 120, which indicates that the halite had undergone reaction and did not show up on the XRD patterns. This indicates that RR 120 was adsorbed onto the clay structure surface. Moreover, the main peak at a 2-theta value of approximately 5.898 (d space value of 14.973) disappeared in the reactive mixture of aminoclay and RR 120, which indicates that the clay structure collapsed and contributed to the effective adsorption of RR 120. A 2 : 1 trioctahedral structure at $2\theta=59^{o}$, which corresponds to a smectite reflection, was observed in the organo (phyllo) silicates [33]. Another broad in-plane reflection was identified at $d_{020,110}=0.40$ nm ($2\theta=22.33^{o}$). The thickness of the regularly laid unit clay structure was obtained at d_{001}, where it was measured to be approximately 1.5 nm. In order to confirm the existence of functional adsorption on the Mg-AMP clay, the FT-IR spectra of Mg-AMP clay is presented in Fig. 2. It shows the diffuse reflectance FT-IR spectra of the Mg-AMP clay compound. The characteristic bands of Mg-AMP clay were -CH_2- (3,036 cm^{-1}), -NH^{3+} (2,036 cm^{-1}), -NH_2 (1,604 cm^{-1}), -CH_2 (1,498 cm^{-1}), Si-C (1,141 cm^{-1}), Si-O-Si (1,042 cm^{-1}), and Mg-O (465 cm^{-1}) [34]. The main changes occurred in the region spanning from 2,000 to 400 cm^{-1}. The NH^{3+} peak (2,036 cm^{-1}) disappeared in Fig. 2(c), which shows Mg-AMP clay with anionic contaminants due to interactions between the cationic -NH^{3+} group and the RR 120 dye anion. This result is similar to the previously reported MG (malachite green) dye removal process [33]. The change in band intensity in the FT-IR spectra indicates a possibility of chemical bonds between the Mg-AMP clay and dye molecules in the mixture. SEM and EDX are the best known and most widely used surface analysis techniques. Moreover, EDX elemental analysis has been used to describe chemical compositions. In EDX elemental analysis, the compositions of Mg, Si, and Cl were predominantly detected (Fig. 3).

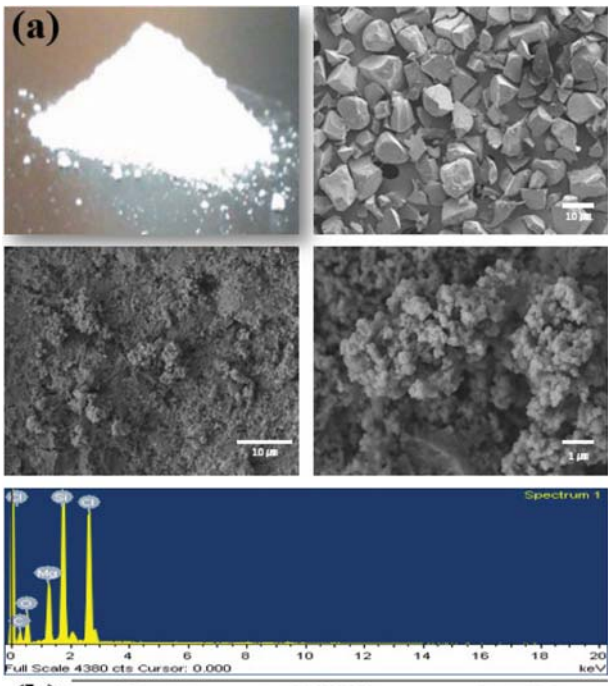

Element	Weight%	Atomic%
C	32.91	48.01
O	25.50	27.93
Mg	6.48	4.67
Si	15.79	9.85
Cl	19.32	9.55
Totals	100.00	

Fig. 3. (a) SEM image and (b) SEM-EDX spectra for Mg-AMP clay powder.

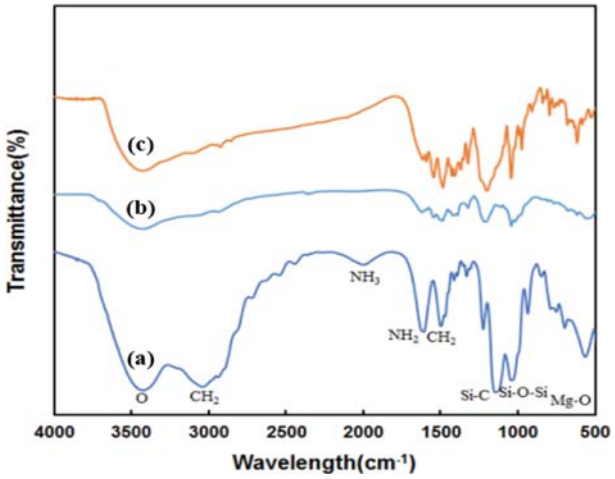

Fig. 2. FT-IR spectra of (a) Mg-AMP clay, (b) RR 120 dye, (c) Mg-AMP clay after adsorption.

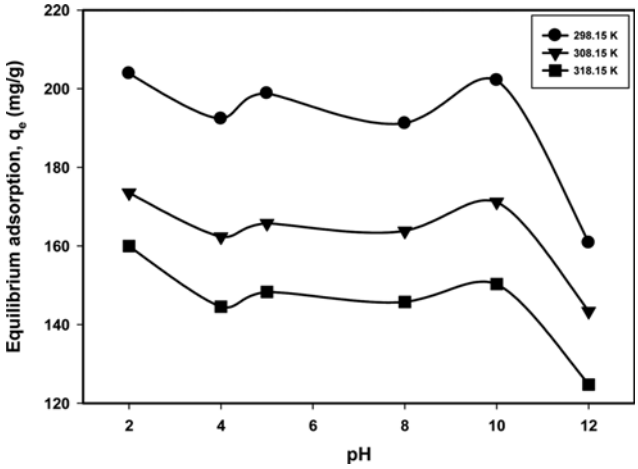

Fig. 4. Effect of pH on the adsorption of RR 120 Mg-AMP clay with an initial concentration of 50 mg/L at 25-45 °C.

2. Effect of pH on RR 120 Removal

The effect of dye solution pH on the adsorption of RR 120 onto Mg-AMP clay adsorbent was studied for pH values of 3-12, at 25-45 °C and 50 mg/L initial dye concentration (Fig. 4). The equilibrium dye-uptake removal capacity was found to be maximum at solution pH values of 2. Lower adsorption of RR 120 at high pH is probably due to the presence of excess OH^- ions, which compete with the SO_3^- and Cl^- groups in the dye. The adsorption of these dye anion or cation charged groups onto the adsorbent surface is mainly influenced by the surface charge on the adsorbent, which in turn is influenced by the solution pH [35]. The previous study reported that the RR 120 dye has the following chemical properties. RR 120 has six sulfonic acid groups and two phenolic OH^- groups near the azo groups as anionic sites [36]. On the other hand, there are two diaminochlorotriazine groups at the cationic sites. The chemical structure is composed of three species of pH solutions. Also, due to the influence of the dye on the pH, the adsorption capacity is increased because the electrostatic interaction between the dye of negative charge and the adsorbent of positive charge is increased.

3. Adsorption Isotherms

The Langmuir and Freundlich isotherm adsorption equations were applied to analyse the relation between RR 120 and Mg-AMP clay (Fig. 5). The suitability of the model was evaluated by determining the average percentage error. For an Mg-AMP clay dosage of 10 mg/mL, the Langmuir model obtained maximum adsorption capacities of 229.94, 182.26, and 156.54 mg/g at 298.15, 308.15, and 318.15 K. The results are shown in Table 3. The Langmuir model indicated that the maximum adsorption capacity of RR 120 increases as the temperature is decreased. Furthermore, the results show a higher correlation average percentage error. The removal effect of various non-clay adsorbents on RR 120 was compared with that of Mg-AMP clay. It can be seen from Table 6 that the adsorption capacity of Mg-AMP clay obtained in this experiment is much higher than that of the other adsorbents. Clay has a high specific surface area and the adsorption process is advantageous, because it has a charge on the surface. The absorbents are classified as clay and non-clay. In the case of clay, Fouchana clay consists of a 10% interstratified lite/semectite and 50% smectite. The amount of clay that adsorbs RR 120 is less, because its molecule size is bigger than that is capable of being inserted into the inner layer [37]. The other clays also seem to have a similar mechanism. However, Mg-AMP clay has higher absorption capacity because of its nature (exfoliated and intercalated). In contrast, chitosan nanodispersion [11], Amberlite IRA-900 resin [12], Chitosan-Fe exhibited higher adsorption capacity than the Mg-AMP clay [38]. Chitosan nanodispersion showed high adsorption capacity than cationic surface nanodispersion, which was partially neutralized by STPP; the positively charged nanoparticles act as an effective flocculant because the dye is a multivalent anion [11]. In the case of Amberlite IRA-900 resin, there is an increased adsorption of dye molecules, due to the adsorption by the internal surface (by pore diffusion) after the adsorption by the external surface reached saturation [12].

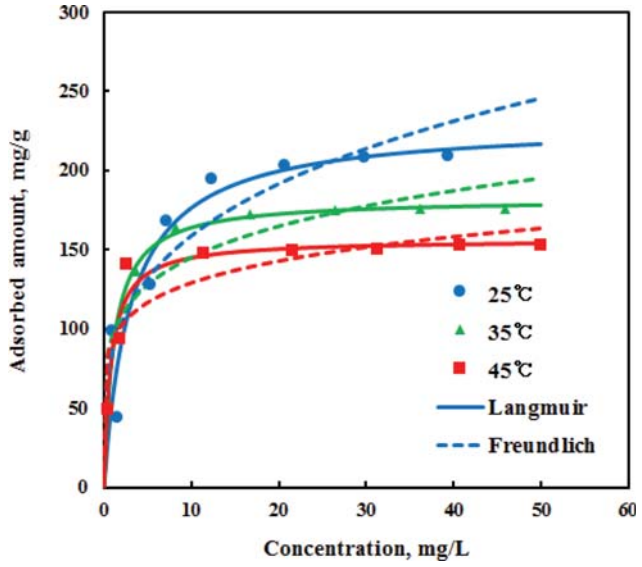

Fig. 5. Langmuir and Freundlich Isotherm constants for adsorption of RR 120 dye on Mg-AMP clay at different temperatures.

4. Adsorption Thermodynamics

The thermodynamic parameter results are shown in Table 4. The calculated ΔG^o values varied from −50.38 to −53.76, when the temperature was increased from 298 K to 318 K. The positive values of ΔS^o and ΔH^o are in contrast with the negative values of ΔG^o. The negative values of ΔG^o indicate that RR 120 adsorption is spontaneous. Moreover, the system does not gain energy from an external source. In contrast, the positive value of ΔS^o indicates the increased degree of freedom of the system. Likewise, the positive value of ΔH^o indicates that the reaction between RR 120 and Mg-AMP clay is endothermic.

5. Adsorption Kinetics

As shown in Fig. 6, the estimated values of q_e and k_1 for the pseudo first-order model were 85.24 mg/g and 0.087 min^{-1}, and the values of q_e and k_2 for the pseudo second-order model were

Table 3. Study of temperature on the adsorption isotherms of the dye RR 120

Langmuir equation $q_e=q_m bC_e/(1+bC_e)$				Freundlich equation $q_e=K_F C_e^{1/n}$		
T (K)	q_m (mg/g)	b	E* (%)	K_F	n	E (%)
298.15	229.94	0.33	0.87	84.78	0.27	0.82
308.15	182.26	0.90	0.99	95.04	0.18	0.85
318.15	156.54	1.26	0.93	92.20	0.15	0.73

*Average percent error: $E(\%)=\frac{100}{n}\Sigma_{k=1}^{n}\left[\frac{q_{exp,k}-q_{cal,k}}{q_{exp,k}}\right]$

Table 4. Thermodynamic parameters of Mg-AMP clay

ΔG^o (kJ/mol)			ΔH^o (kJ/mol)	ΔS^o (kJ/mol)
293.15 K	303.15 K	313.15 K		
−50.38	−52.07	−53.76	52.92	169.14

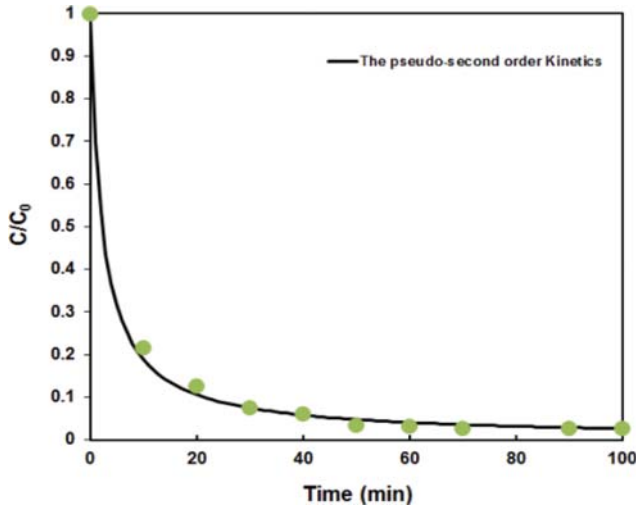

Fig. 6. Adsorption kinetics fitted by pseudo-second-order equation.

Table 5. Kinetic parameters of RR 120 dye adsorption on Mg-AMP clay

Pseudo-first order			Pseudo-second order		
k_1 (min^{-1})	q_e (mg/g)	R^2	k_2 (g/mg min^{-1})	q_e (mg/g)	R^2
0.09	85.24	0.97	0.00	124.59	1.00

Table 6. Comparison of adsorption capacities of various sorbents for RR 120

Classification	Adsorbent	q_e (mg/g)	Refs.
Clay	**Mg-AMP clay**	**229.9**	**In this study**
	Fouchana clay+HDTMA[a]	163.9	[50]
	CPC-bentonite[b]	81.9	[51]
	Fouchana clay	54.6	[15]
	Fouchana clay	29.9	[16]
Non-clay	Chitosan nanodispersion	910.0	[11]
	Amberlite IRA-900 resin[c]	692.3	[12]
	Chitosan-Fe	290.9	[38]
	Fe_3O_4 magnetic nanoparticles	166.7	[13]
	Oxygen furnace slag-BTA[d]	84.5	[14]
	Oxygen furnace slag-BTM[e]	44.1	[14]

[a]HDTMA: Hexadecyltrimethylam-monium bromide
[b]CPC-bentonite: Na-bentonite with cetylpyridinium chloride (CPC)
[c]Amberlite IRA-900: Anion exchangers based oh the styrene-dibinylebenzene
[d]BTA: Basic oxygen furnace slag treated by acid
[e]BTM: Basic oxygen furnace slag treated by milling

124.59 mg/g and 0.0035 g/mg min^{-1}. The data parameters evaluated with the kinetic equation and correlation coefficient are shown in Table 5. These values indicate that the pseudo-second-order equation fitted well with the pseudo-first-order equation for the adsorption of RR 120 using Mg-AMP clay.

6. Large-scale Synthesis of Mg-AMP Clay

Large-scale Mg-AMP clay synthesis is performed for a large-scale implementation of clay for RR 120 removal. The experiment was carried out by adding 200 times the conventional amount for synthesis to the 10 L reactor. The yield for the synthesis with the small amount was 96%, while the yield for large-scale synthesis was 80%. There was no structural difference between the mass synthesis and small amount synthesis. In the synthesis method, it is possible to control the functionality and yield by controlling the molecular ratio of two or more organosilanes having different functional groups. Owing to this feature, our large synthesis strategy using bulk chemical reactor is highly promising as an efficient method for mass-production of Mg-AMP clay. In previous studies, the potential toxicity of oragnoclay in the cell experiment with Mg-AMP clay has been reported [39]. Consequently, organoclay may be exposed to the environment, or human body. Besides, the organic clay affects not only the adsorption of dyes but also the encapsulating proteins, gene transfer, or drug delivery [40,41]. Mg-AMP clay was more efficient in removing the hazardous material, dye malachite green. Due to this result, Mg-AMP clay can be used as an eco-friendly material. The large-scale study is under way in the laboratory, Chosun University.

DISCUSSION

Natural clay has the characteristic of a negatively charged surface [36]. However, Mg-AMP clay has a positively charged surface. According to the paper by Lee et al., Mg-AMP clay has an adsorption property due to the electrostatic interaction with the anions of a metal [34]. In addition, the organic building block of Mg-AMP clay can be precipitated by exfoliation and intercalation. Therefore, it has excellent adsorption capacity in anion-charged metals [41], lipids [43], DNA [44], and enzymes [20]. From the experiment with RR 120 and Mg-AMP clay flocculation in an aqueous solution system, it is seen that there is an electrostatic attraction between the positively charged NH^{3+} of Mg-AMP clay and the negatively charged SO^{3-} of RR 120. A phenomenological analysis is that of a strong force between Mg-AMP clay sheets and RR 120 dye molecules. It is determined as a result of the chemically detected precipitation from the bottom of the solution. XRD, FT-IR, and EDX were used to determine the precipitation dye molecules that were formed and the Mg-AMP clay sheet composition of the Si-O-Mg collapsed structure. As mentioned above, Mg-AMP clay consists of amine groups covalently attached to the backbone of magnesium ions. Research on Mg-AMP clay was started by Mann and his colleagues [45]. According to them, the organoclay as 2 : 1 trioctagedral typed aminopropyl magnesium phyllosilicate. In addition, the clay minerals of layered organo-inorganic hybrid materials resemble the talc like structure $Si_8Mg_6O_{20}(OH)_4$ with $MgCl_2$ and 3-aminopropyl triethoxysilane (APTES) [46]. According to the XRF instrumental analysis results of Mg-AMP clay, the Mg-AMP clay is

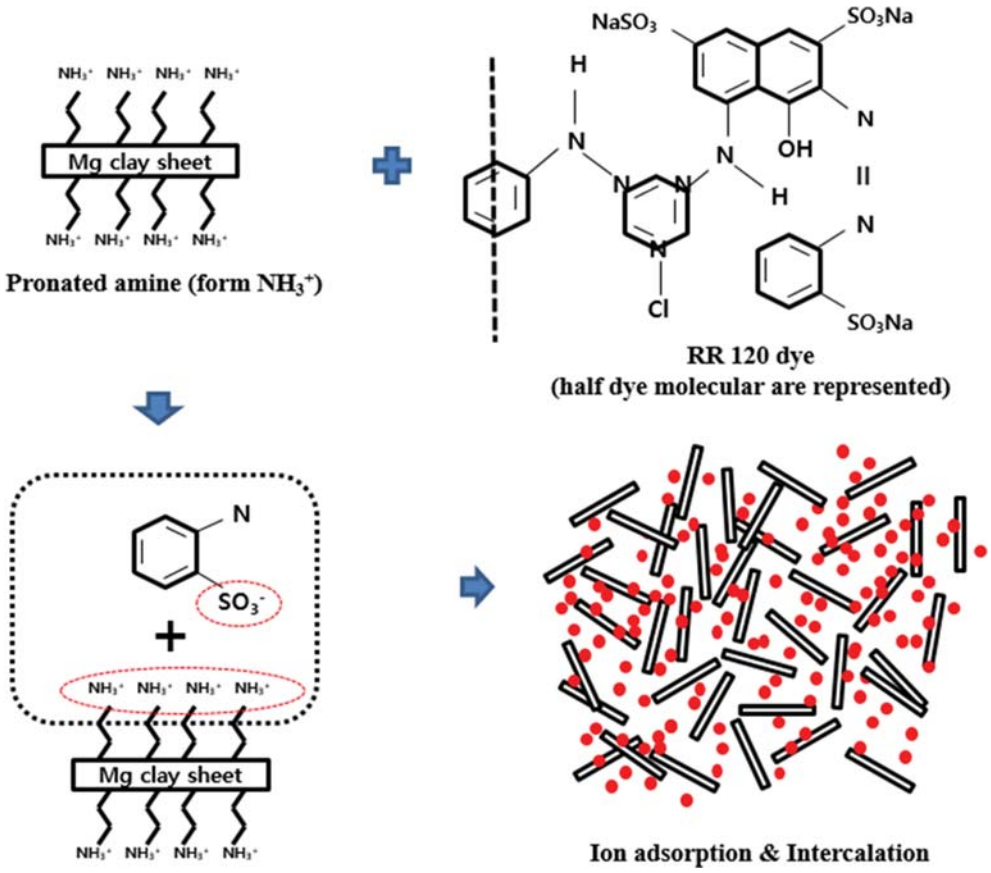

Fig. 7. Schematic representation of the adsorption mechanism of RR 120 by Mg-AMP clay.

mostly composed of MgO (22.9 wt%) and SiO_2 (72.2 wt%). These results reveal the validity of the Mg-AMP clay structure. For this reason, the functional group RNH_2 of Mg-AMP clay on the surface formed protonated amine ($R\text{-}NH_3^+$) and water. In addition, the ultrasonic treatment allows the clay sheets to be exfoliated. The pronated amine is promotive of adsorption due to the exfoliated Mg-AMP clay sheets. Thus, the basic dye structure is negatively charged with six sulfonate groups on the exfoliated sheets [36]. Making the exfoliated sheet is important, because it increases the adsorption capacity, forming big Mg-AMP clay sheet nets. The exfoliated Mg-AMP clay sheets perform rapid precipitation [24,47]. According to the scheme, the dye molecule is precipitated on the clay sheet and the structure of Mg-AMP clay is collapsed. This mechanism is confirmed by the instrumental analysis shown in Fig. 7. In the RR 120 and Mg-AMP clay precipitation in aqueous system, the electrostatic attraction between positively charged NH^{3+} of Mg-AMP clay and negatively charged SO^{3-} of RR 120 occurs. The Mg-AMP clay and RR 120 molecules act as electron donor and acceptor, respectively, via van der Waals forces and electrostatic interactions. The electrostatic attraction as well as exfoliation and intercalation are considered to be the most important of these mechanisms. In the case of desorption of Mg-AMP clay and dye, separation cost is higher and it is good to use for simple dye removal. In contrast, it is preferable to recover high value-added substances such as metal ions, chlorella [48], microalgae and lipids [49].

CONCLUSIONS

Nano-sized aminopropyl magnesium phyllosilicates (Mg-AMP clay) were easily synthesized in large quantities and an adsorption study was performed using this clay to remove Reactive Red 120. The appropriate adsorption model was a Langmuir model and the kinetics were elucidated under the operation conditions. In addition, the removal efficiency of RR 120 was studied using UV-Vis spectrophotometer, XRD, FT-IR, XRF, SEM, and EDX techniques. Removal mechanism of RR 120 using Mg-AMP clay was suggested through adsorption and precipitation phenomena. Since the large-scale production of Mg-AMP clay is possible and economically feasible, an appropriate removal methodology should be considered in advance using Mg-AMP clay as a control scheme for harmful wastewater containing dye component.

ACKNOWLEDGEMENT

This work was supported by the research fund from Chosun University, 2016.

REFERENCES

1. I. M. Banat, P. Nigam, D. Singh and R. Marchant, *Bioresour. Technol.*, **58**, 217 (1996).
2. P. A. Carneiro, G. A. Umbuzeiro, D. P. Oliveira and M. V. B. Zanoni,

J. Hazard. Mater., **174**, 694 (2010).
3. X.-Y. Yang and B. Al-Duri, *Chem. Eng. J.*, **83**, 15 (2001).
4. N. F. Cardoso, E. C. Lima, B. Royer, M. V. Bach, G. L. Dotto, L. A. Pinto and T. Calvete, *J. Hazard. Mater.*, **241**, 146 (2012).
5. R. Gong, M. Li, C. Yang, Y. Sun and J. Chen, *J. Hazard. Mater.*, **121**, 247 (2005).
6. D. S. Brookstein, *Dermatol. Clin.*, **27**, 309 (2009).
7. V. S. Houk, *Mutat. Res. Rev. Genet. Toxicol.*, **277**, 91 (1992).
8. G. Crini, *Bioresour. Technol.*, **97**, 1061 (2006).
9. G. Crini and P.-M. Badot, *Prog. Polym. Sci.*, **33**, 399 (2008).
10. R. B. Venkata and C. A. Sastray, *Indian J. Environ. Prot.*, **7**, 363 (1987).
11. H. Momenzadeh, A. R. Tehrani-Bagha, A. Khosravi, K. Gharanjig and K. Holmberg, *Desalination*, **271**, 225 (2011).
12. M. Greluk and Z. Hubicki, *Chem. Eng. Res. Des.*, **91**, 1343 (2013).
13. G. Absalan, M. Asadi, S. Kamran, L. Sheikhian and D. M. Goltz, *J. Hazard. Mater.*, **192**, 476 (2011).
14. Y. Xue, H. Hou and S. Zhu, *Chem. Eng. J.*, **147**, 272 (2009).
15. N. Abidi, E. Errais, J. Duplay, A. Berez, A. Jrad, G. Schäfer, M. Ghazi, K. Semhi and M. Trabelsi-Ayadi, *J. Clean. Prod.*, **86**, 432 (2015).
16. E. Errais, J. Duplay, F. Darragi, I. M'Rabet, A. Aubert, F. Huber and G. Morvan, *Desalination*, **275**, 74 (2011).
17. S. Babel and T. A. Kurniawan, *J. Hazard. Mater.*, **97**, 219 (2003).
18. H. A. Patel, R. S. Somani, H. C. Bajaj and R. V. Jasra, *Bull. Mater. Sci.*, **29**, 133 (2006).
19. M. Okamoto, S. Morita, H. Taguchi, Y. H. Kim, T. Kotaka and H. Tateyama, *Polymer*, **41**, 3887 (2000).
20. A. J. Patil and S. Mann, *J. Mater. Chem.*, **18**, 4605 (2008).
21. M. A. Melo Jr., F. J. B. E. Oliveira and C. Airoldi, *Appl. Clay Sci.*, **42**, 130 (2008).
22. Y.-C. Lee, W.-K. Park and J.-W. Yang, *J. Hazard. Mater.*, **190**, 652 (2011).
23. H.-K. Han, Y.-C. Lee, M.-Y. Lee, A. J. Patil and H.-J. Shin, *ACS. Appl. Mater. Inter.*, **3**, 2564 (2011).
24. V. K. H. Bui, D. Park and Y.-C. Lee, *Chem. Eng. J.*, **336**, 757 (2018).
25. A. J. Patil, E. Muthusamy and S. Mann, *Angew. Chem. Int. Ed.*, **43**, 4928 (2004).
26. A. J. Patil, E. Muthusamy and S. Mann, *J. Mater. Chem.*, **15**, 3838 (2005).
27. Y.-C. Lee, T.-H. Lee, H.-K. Han, W. J. Go, J.-W. Yang and H.-J. Shin, *Photochem. Photobiol.*, **86**, 520 (2010).
28. I. Langmuir, *J. Am. Chem. Soc.*, **38**, 2221 (1916).
29. H. M. F. Freundlich, *J. Phys. Chem.*, **57**, 385 (1906).
30. D. S. Abrams and J. M. Prausnitz, *AIChE J.*, **21**, 116 (1975).
31. S. Lagergren, *Handlingar*, **24**, 1 (1898).
32. Y.-S. Ho and G. McKay, *Process Biochem.*, **34**, 451 (1999).
33. Y.-C. Lee, E. J. Kim, J.-W. Yang and H.-J. Shin, *J. Hazard. Mater.*, **192**, 62 (2011).
34. Y.-C. Lee, W.-K. Park and J.-W. Yang, *J. Hazard. Mater.*, **190**, 652 (2011).
35. K. Didehban, M. Hayasi and F. Kermajani, *Korean J. Chem. Eng.*, **34**, 1177 (2017).
36. E. Errais, J. Duplay, M. Elhabiri, M. Khodja, R. Ocampo, R. Baltenweck-Guyot and F. Darragi, *Colloid. Surface. A.*, **403**, 69 (2012).
37. L. B. De Paiva, A. R. Morales and F. R. V. Díaz, *Appl. Clay Sci.*, **42**, 8 (2008).
38. C. A. Demarchi, M. Campos and C. A. Rodrigues, *J. Environ. Chem. Eng.*, **1**, 1350 (2013).
39. G. Chandrasekaran, H.-K. Han, G.-J. Kim and H.-J. Shin, *Appl. Clay Sci.*, **53**, 729 (2011).
40. A. J. Patil, M. Li and S. Mann, *Nanoscale*, **5**, 7161 (2013).
41. C. Viseras, P. Cerezo, R. Sanchez, I. Salcedo and C. Aguzzi, *Appl. Clay Sci.*, **48**, 291 (2010).
42. Y.-C. Lee, E. J. Kim, H.-J. Shin, M. Choi and J.-W. Yang, *J. Ind. Eng. Chem.*, **18**, 871 (2012).
43. A. J. Patil, E. Muthusamy, A. M. Seddon and S. Mann, *Adv. Mater.*, **15**, 1816 (2003).
44. A. J. Patil, M. Li, E. Dujardin and S. Mann, *Nano Lett.*, **7**, 2660 (2007).
45. S. L. Burkett, A. Press and S. Mann, *Chem. Mater.*, **9**, 1071 (1997).
46. S. Mann, S. L. Burkett, S. A. Davis, C. E. Fowler, N. H. Mendelson, S. D. Sims, D. Walsh and N. T. Whilton, *Chem. Mater.*, **9**, 2300 (1997).
47. Y.-C. Lee, J.-Y. Kim and H.-J. Shin, *Sep. Sci. Technol.*, **48**, 1093 (2013).
48. Y.-C. Lee, B. Kim, W. Farooq, J. Chung, J.-I. Han, H.-J. Shin, S. H. Jeong, J.-Y. Park, J.-S. Lee and Y.-K. Oh, *Bioresour. Technol.*, **132**, 440 (2013).
49. W. Farooq, Y.-C. Lee, J.-I. Han, C. H. Darpito, M. Choi and J.-W. Yang, *Green Chem.*, **15**, 749 (2013).
50. A. Nejib, D. Joelle, A. Fadhila, G. Sophie and T.-A. Malika, *Desalin. Water. Treat.*, **54**, 1754 (2015).
51. A. Tabak, N. Baltas, B. Afsin, M. Emirik, B. Caglar and E. Eren, *J. Chem. Technol. Biotechnol.*, **85**, 1199 (2010).